The c-Myc Oncogene Directly Induces the H19 Noncoding RNA by Allele-Specific Binding to Potentiate Tumorigenesis

Dalia Barsyte-Lovejoy,[1] Suzanne K. Lau,[3,4] Paul C. Boutros,[1,2,4] Fereshteh Khosravi,[1] Igor Jurisica,[2,4,6] Irene L. Andrulis,[7] Ming S. Tsao,[3,4,5] and Linda Z. Penn[1,4]

Divisions of [1]Cancer Genomics and Proteomics, [2]Signaling Biology, and [3]Applied Molecular Oncology, Ontario Cancer Institute/Princess Margaret Hospital; Departments of [4]Medical Biophysics and [5]Laboratory Medicine and Pathobiology, [6]Computer Science, University of Toronto, Canada; and [7]Fred Litwin Cancer Genetics Center, Samuel Lunenfeld Research Institute Mount Sinai Hospital, Toronto, Ontario, Canada

Abstract

The product of the *MYC* oncogene is widely deregulated in cancer and functions as a regulator of gene transcription. Despite an extensive profile of regulated genes, the transcriptional targets of c-Myc essential for transformation remain unclear. In this study, we show that c-Myc significantly induces the expression of the *H19* noncoding RNA in diverse cell types, including breast epithelial, glioblastoma, and fibroblast cells. c-Myc binds to evolutionarily conserved E-boxes near the imprinting control region to facilitate histone acetylation and transcriptional initiation of the *H19* promoter. In addition, c-Myc down-regulates the expression of insulin-like growth factor 2 (*IGF2*), the reciprocally imprinted gene at the *H19/IGF2* locus. We show that c-Myc regulates these two genes independently and does not affect *H19* imprinting. Indeed, allele-specific chromatin immunoprecipitation and expression analyses indicate that c-Myc binds and drives the expression of only the maternal *H19* allele. The role of H19 in transformation is addressed using a knockdown approach and shows that down-regulation of H19 significantly decreases breast and lung cancer cell clonogenicity and anchorage-independent growth. In addition, c-Myc and H19 expression shows strong association in primary breast and lung carcinomas. This work indicates that c-Myc induction of the *H19* gene product holds an important role in transformation. (Cancer Res 2006; 66(10): 5330-7)

Introduction

The transforming members of the Myc family (c-Myc, N-Myc, and L-Myc) show deregulated expression in a broad spectrum of cancers, including carcinomas of the lung, breast, and prostate as well as leukemias and lymphomas (1). c-Myc is a transcription factor that, with its obligate heterodimerization partner Max, binds to DNA sequence elements called E-boxes (2). c-Myc-Max can subsequently recruit histone acetyltransferase (HAT) activity (3), chromatin remodeling complexes (4), or promote RNA polymerase II (RNAPII) clearance (5) to allow for target gene transcription. c-Myc-Max can also repress gene transcription primarily by interfering with the assembly or function of the transcriptional complex (6–8). As a transcription factor, c-Myc regulates numerous gene targets that subsequently execute its many biological activities, including cell proliferation, transformation, angiogenesis, and apoptosis (9). Identifying these target genes is key in elucidating the role of this potent oncogene in transformation and has thus received much attention. Despite an extensive list of c-Myc-regulated genes, it remains unclear which cohort of target genes is responsible for the strong transforming activity of c-Myc (10, 11).

Recent analyses using advanced high-throughput chromatin immunoprecipitation technology has revealed the nature of the target genes whose promoter regulatory regions are bound by c-Myc (12–15). Remarkably, these analyses have indicated that c-Myc target genes include both coding and noncoding RNAs (ncRNA; ref. 16). Noncoding RNAs are transcripts expressed and processed in the nucleus in a manner similar to protein coding genes; however, ncRNAs lack a conserved open reading frame. Although elucidating the function of ncRNAs is in the early stages of investigation, evidence suggests that at least some may have roles in tumorigenesis (17). To determine the role of c-Myc-regulated ncRNAs in transformation, we investigated both the regulation and function of the large prototypic ncRNA, H19, as a downstream target of c-Myc.

H19 was first described as a tumor suppressor (18, 19), but more recent analysis shows that H19 expression is reactivated in breast (20), endometrial (21), lung (22), cervical (23), esophageal (24), and bladder (25) tumors. The *H19*/insulin-like growth factor 2 (*IGF2*) locus, containing both the *H19* and *IGF2* genes, is subject to genomic imprinting, which leads to differential allelic expression of H19 from the maternal allele and IGF2 from the paternal allele (26). This allele-specific expression is highly regulated by differential methylation of CpG dinucleotides that are usually concentrated in CpG islands, genomic elements that are often located close to promoter regions (27). As our data indicated that c-Myc can bind to intergenic regions containing CpG islands (13), we also explored the consequences of allele-specific CpG methylation on the transcriptional regulatory function of c-Myc at the *H19/IGF2* locus.

In this study, we show that c-Myc induces the expression of the H19 ncRNA and binds directly to E-boxes close to the imprinting control region (ICR). Using allele-specific chromatin immunoprecipitation analysis, we show that c-Myc specifically binds and regulates the active maternal *H19* allele and does not bind or affect the expression of the silenced paternal allele. In addition, c-Myc down-regulates transcription of the reciprocally imprinted gene *IGF2*. The significance of H19 up-regulation by c-Myc and the association of c-Myc and H19 transcript levels were assessed in primary and established tumor cells derived from breast and lung cancer patients.

Note: Supplementary data for this article are available at Cancer Research Online (http://cancerres.aacrjournals.org/).

Requests for reprints: Linda Z. Penn, Division of Cancer Genomics and Proteomics, Ontario Cancer Institute/Princess Margaret Hospital, 610 University Avenue, Toronto, Canada M5G 2M9. Phone: 416-946-2276; Fax: 416-946-2840; E-mail: lpenn@uhnres.utoronto.ca.

doi:10.1158/0008-5472.CAN-06-0037

Materials and Methods

Cell lines. The immortal, nontransformed MCF10A breast cell line (gift from Dr. Muthuswamy) was cultured as described (28). Cells were grown with 10% fetal bovine serum in α-MEM (glioblastoma T98G), DMEM H21 (rat cardiomyocyte H9C2 and fibroblast Rat1MycER^{TAM}), McCoy's (breast cancer cell lines MDA-MB231, SKBR3, and colon carcinoma line HCT116), and RPMI 1640 (T47D breast cancer cell line and lung cancer cell lines A549, H460, and H520). Rat Myc null cells (HO15.19) were grown in DMEM H21 with 10% calf serum. Where indicated, 5 μmol/L 5-aza-deoxycytidine (AzaC; Sigma, St. Louis, MO) was added to cells every 24 hours. Trichostatin A (TSA; Calbiochem, La Jolla, CA) was used at 300 nmol/L.

Retroviral gene transfer. Ectopic human c-Myc was introduced by infection with ecotropic, replication-incompetent retrovirus, and expression was confirmed as described (29).

Isolation and analysis of RNA. Total RNA was isolated as previously described (30) and purified using the RNeasy Mini kit (Qiagen, Inc., Chatsworth, CA). Five micrograms of total cellular RNA were reverse transcribed using Superscript II Reverse Transcription reagents and OligoD_T (Invitrogen, San Diego, CA). Northern blots were done as described (11).

Gene expression analysis in cancer cell lines. Semiquantitative reverse transcription-PCR (RT-PCR) was carried out as described (13) with primers provided in Supplementary Table S1, and the conditions are available upon request. For the quantitative real-time RT-PCR analysis of the breast and lung cell lines, SYBR Green PCR Master Mix (Applied Biosystems, Foster City, CA) were used according to the manufacturer's instructions. A total of one thousandth of the cDNA reaction was used for each PCR triplicate. The results were normalized to the levels of the 36B4 transcript using the comparative C_t method. The allele-specific PCR employed the forward primers specific for the particular *H19* allele, CGGCTCTCGAAGGTGAAGCT (B) or CGGCTCTCGAAGGTGAAGCG (A), and the reverse primer used was TCGTGGAGGCTTTGAATCTCTCAG.

Selection of patients. The RNA expression profiles of a total of 186 breast cancer samples, representing 137 distinct tumors from the cohort described (31), were assayed using cDNA expression microarrays. Two samples lacked follow-up data and were excluded from further analysis. A total of 240 snap-frozen non–small cell lung (NSCLC) carcinoma samples were harvested from patients who have been treated primarily by surgical resection at the University Health Network from 1996 to 2000. Tissues were banked with informed consent, and the studies have been approved by the institutional Research Ethics Board.

Analysis of breast tumor expression data. Raw microarray images were quantitated with the GenePix (Axon, Union City, CA) software package with flagging of low-quality spots. Spot signal was calculated by subtracting the median background pixel intensity from the mean foreground pixel intensity. Ratios were transformed into $\log_2$ space, and missing values were imputed from spotwise duplicates where possible. Data were normalized by sequential print-tip loess smoothing (within array) and scale adjustment (between arrays) as described by Yang et al. (32). All normalization employed the limma package of the Bioconductor library for R (v 2.0.1; ref. 33). Normalized expression values were centered using a 15% trimmed mean. To assess the spot quality, we determined the correlation of the two sequences representing H19 (BI092679 and BQ028553) and MYC (H43827 and W87741). Five outliers with extreme *H19* expression were identified via the *Q* test and removed, leading to higher spot correlation ($R = 0.72$). Spots were then collapsed by averaging. Similarly, the expression from two MYC spots were found to be largely uncorrelated ($R = -0.07$); thus, the clone most specific to MYC was selected. These normalized data represented 137 distinct tumor samples, with clinical follow-up available for 135 of these. These samples were dichotomized around the median H19 expression level. A *t* test with the assumption of unequal variances was used to test MYC expression for significant differences. Normalized array data for all spots are available as Supplementary Table S2.

Quantification and analysis of *MYC* and *H19* expression in lung tumor samples. Real-time quantitative PCR amplification was conducted using the SYBR Green assay in the ABI PRISM 7900-HT (Applied Biosystems). Each 10-μL quantitative RT-PCR reaction contained a 2-ng equivalent of cDNA in a 384-well plate. The reactions were activated at 95°C for 3 minutes followed by 40 cycles of 95°C for 15 seconds, 65°C for 15 seconds, and 72°C for 20 seconds. The transcript number/ng cDNA was obtained using standard curves generated with a pool of 10 nontumor lung genomic DNAs. Primer sequences are provided in Supplementary Table S1. Duplicate RT samples were used in each assay. Technical replicates displayed high correlation ($R_{avg} = 0.96 \pm 0.04$; Supplementary Fig. S1) and were then collapsed through averaging. First, expression values were $\log_2$ transformed after addition of a pseudocount. Samples lacking H19 or TBP signal were removed from the data set. For each of the remaining samples, a normalization factor was calculated using the mean of the four housekeeping genes (*TBP, ACTB, B2M*, and *BAT1*) and used to remove nonbiologicalvariability.Forthe*i*thpatient,thenormalizationfactoris N_i $N_i = 0.25 \times [X_i(\text{TBP}) + X_i(\text{ACTB}) + X_i(\text{B2M}) + X_i(\text{BAT1})]$, and normalized expression values for gene M are $Y_i(M) = X_i(M) - N_i$, where the X_i values correspond to unnormalized expression values. For each patient cohort, the normalized expression values were median centered to yield the final expression estimates: $Z_i(M) = Y_i(M) - \text{median}[Y(M)]$. The two patient cohorts were then merged, and the overall data set of 240 distinct samples was dichotomized around the median H19 expression level. A *t* test with the assumption of unequal variances was used to test for differential c-Myc expression. Raw quantitative RT-PCR data are available online as Supplementary Table S3.

Chromatin immunoprecipitation. Chromatin immunoprecipitation was done as previously described (13) using the following antibodies: 2 μg Myc (Sc-764), 1 μg CTCF, 0.5 μg RNAPII (Sc-764), 1 μg Max, all from Santa Cruz Biotechnology (Santa Cruz, CA), and 0.5 μg of AcH3 or AcH4 (Upstate Biotechnology, Lake Placid, NY). Real-time PCR was done as described above using human genomic DNA as the standard and normalizing the specific antibody signal to the input signal. Primer sequences are provided in the Supplementary Table S1, and the conditions are available upon request. The same chromatin immunoprecipitation material was used for allele specific PCR with allele-specific primers CGCCTACTTATGTGATGATCAG or CGCCTACTTATCTGATGATCAC and the reverse GCACCCACGATAATGGATT.

H19 knockdown. The small interfering RNAs (siRNA) were designed using the SFold web site (http://sfold.wadsworth.org). The control siRNA was against luciferase (34), whereas H19 hairpin oligo sequences are CCGGGCGGGTCTGTTTCTTTACTTTCAAGAGAAGTAAAGAAACAGACC-CGCTTTTTG and reverse AATTCAAAAAGCGGGTCTGTTTCTTTACTTCT-CTTGAAGTAAAGAAACAGACCCGC. The annealed phosphorylated oligos were cloned into pLKO1puro lentiviral vector (gift from Drs. Stewart, Novina, and Weinberg). These constructs, together with packaging vectors pMD.G, pMDLg/pRRE and pRsv-Rev (gift from Dr. Naldini), were transfected into 293TV cells, and viral supernatant was collected 48 hours later and used to infect the cells.

Anchorage and clonogenicity assays. Anchorage-independent growth assays were done as described (29), except 5,000 cells were seeded and counted at the end of a 2-week period. For clonogenicity assays, 500 cells were seeded in six-well dishes, and the media containing puromycin was changed every 3 days. After the 1- to 2-week period, the resulting colonies were stained with 2% methylene blue in 50% ethanol and counted.

Results

c-Myc up-regulates H19 and down-regulates IGF2 transcripts. The *H19/IGF2* locus is subject to genomic imprinting (Fig. 1*A*). Allele-specific methylation of CpG dinucleotides in the ICR leads to H19 expression from the maternal allele, whereas the reciprocally imprinted *IGF2* gene is expressed from the paternal allele (26). The ICR on the maternal allele is unmethylated and bound by CTCF, a zinc-finger protein that acts as a boundary between the enhancers located 3′ of H19 and the promoters of IGF2. The paternal allele is methylated at the ICR, preventing

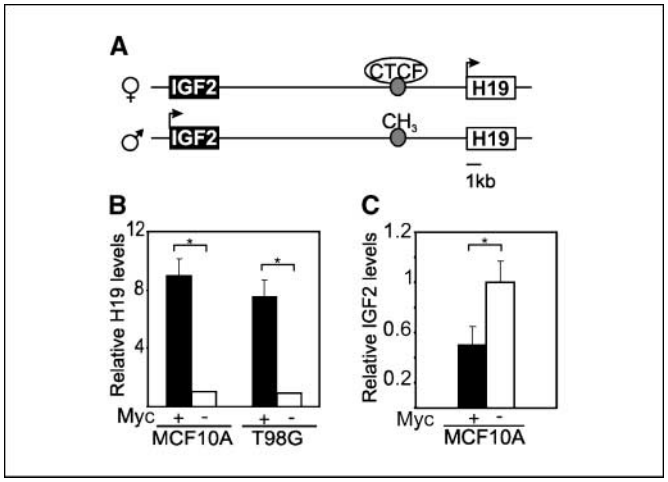

Figure 1. Ectopic Myc induces the expression of H19 and represses IGF2 expression. *A,* schematic of the *H19/IGF2* locus, where active promoters are denoted with arrows and the imprinting control region (*gray circles*) is shown bound by CTCF or methylated (CH_3). *B,* H19 ncRNA expression in MCF10A and T98G cells with (+) and without (−) ectopic Myc as assessed by quantitative RT-PCR. 36B4 ribosomal protein mRNA was used as a normalization control. *C,* IGF2 mRNA levels in MCF10A cells. Quantitative RT-PCR was conducted in triplicates twice. *Columns,* mean; *bars,* SD. *, $P < 0.05$, statistical significance as assessed using a paired *t* test.

CTCF binding, allowing the enhancers to potentiate IGF2 transcription (26).

To evaluate whether c-Myc regulates *H19* expression, we introduced ectopic c-Myc into several cell types, including MCF10A immortalized nontransformed mammary epithelial cells and T98G glioblastoma cells (Supplementary Fig. S2A). Cells with ectopic c-Myc expression showed 7- to 10-fold up-regulation of H19 ncRNA expression as assessed by real-time quantitative RT-PCR (Fig. 1*B*), semiquantitative RT-PCR, and Northern blotting (Supplementary Fig. S2B). This up-regulation was also evident in diploid fibroblasts WI38 (data not shown) and a medulloblastoma cell line UW228 (see Fig. 3*B*). The activation of the constitutively expressed c-Myc/estrogen receptor regulatory region ($MycER^{TAM}$) chimera by 4-hydroxytamoxifen also resulted in elevated H19 expression in Rat-1 fibroblasts (Supplementary Fig. S2C).

Given the strong up-regulation of H19, we assessed the expression of IGF2 in response to exogenous c-Myc expression. Interestingly, c-Myc down-regulated IGF2 in several cell systems, such as MCF10A and WI38 (Fig. 1*C*; data not shown). However, in T98G cells, which have low to undetectable levels of IGF2, down-regulation of IGF2 was not consistently detectable (data not shown). This prompted further evaluation in rat cardiomyocytes that have high basal levels of IGF2 transcripts. c-Myc robustly repressed the levels of IGF2 in H9C2 cardiomyocytes as shown by Northern blot (Supplementary Fig. S2D). Thus, c-Myc strongly up-regulates H19 and down-regulates IGF2 transcript levels in several cell types.

c-Myc directly binds to the regulatory regions of *H19* and *IGF2*. To determine whether c-Myc directly regulates H19, we assessed *in vivo* genomic DNA binding of c-Myc to the regulatory region of H19 using chromatin immunoprecipitation, focusing on the evolutionary conserved E-boxes situated 1.5 and 3.1 kb upstream from the transcription start site. c-Myc immunoprecipitates were highly enriched in these DNA fragments compared with control serum immunoprecipitates (Fig. 2*A*, primer sets 1 and 3). The ICR region containing the second cluster of three DNase hypersensitive sites essential for CTCF binding showed weaker binding of c-Myc (Fig. 2*A*, primer set 2). Interestingly, the abovementioned E-boxes are 650 and 360 bp away from the second hypersensitive site cluster within the ICR, and there are also numerous noncanonical E-boxes interspersed between the

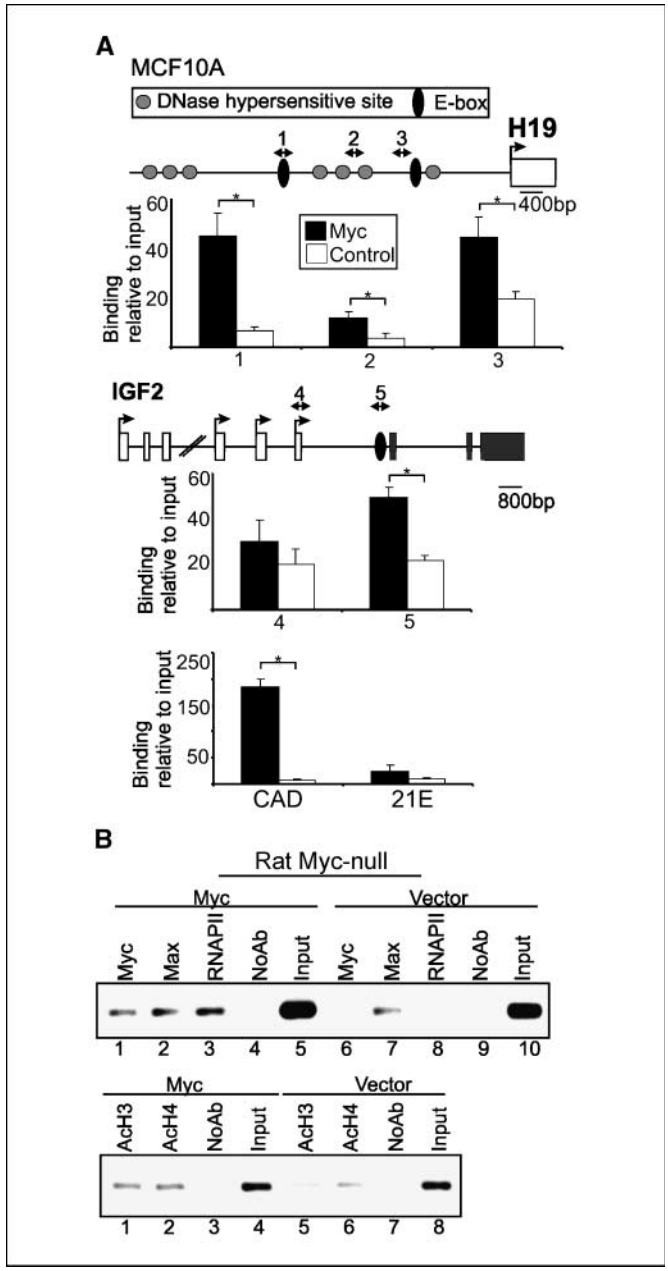

Figure 2. Myc binds to the promoter regions of H19 and IGF2 to regulate gene transcription. *A,* Myc binding at the regulatory region of the *H19* and *IGF2* genes, as well as the CAD (positive control) and chromosome 21 E-box (negative control) was assessed by chromatin immunoprecipitation using Myc-specific antibody (*Myc*) or preimmune serum (*Control*) in MCF10A cells expressing ectopic Myc. Primers are indicated by arrows. DNase-hypersensitive sites (*gray circles*) comprise the ICR. Relative binding was normalized to the input signal and expressed as 0.001% of input. Quantitative PCR was conducted in triplicates twice. *Columns,* mean; *bars,* SD. *, $P < 0.05$, statistical significance as assessed using a paired *t* test. *B,* the transcriptional components bound at the *H19* promoter were assessed by chromatin immunoprecipitation using primers to the proximal E-box (equivalent to primer set 3 in *A*). Rat Myc-null cells that were reconstituted with Myc (*Myc*) or control green fluorescent protein vector (*vector*) were assayed using indicated antibodies. Chromatin immunoprecipitation experiments were repeated at least twice with representative gels shown.

hypersensitive sites. Therefore, from the binding data alone it remained unclear whether Myc would regulate the promoter of H19 or the ICR and imprinting. This issue is addressed through functional analysis below. We have also investigated c-Myc binding to the *IGF2* gene using a scanning chromatin immunoprecipitation approach. *IGF2* is expressed from the promoter P4 in MCF10A cells (data not shown); however, c-Myc binding was weak or undetectable not only at the P4 promoter but also at several other sites, including the differentially methylated region 1 and the coding region in the exon 9 (Fig. 2*A*, primer set 4; data not shown). Only the E-box 5′ from coding exon 7 showed binding of c-Myc (Fig. 2*A*, primer set 5). The positive control *CAD* promoter was highly enriched in c-Myc immunoprecipitates, whereas the negative control E-box at chromosome 21 showed no significant enrichment (Fig. 2*A*). Thus, c-Myc binds to the regulatory regions of *H19* and *IGF2 in vivo*.

c-Myc recruits HATs to the *H19* promoter. To investigate evolutionary conservation and further assess the mechanism of *H19* transcriptional regulation by c-Myc, we compared rat fibroblast cells that are devoid of Myc expression with those that have been reconstituted with ectopic c-Myc for promoter occupancy by chromatin immunoprecipitation analysis. In the absence of c-Myc, Max is bound to the *H19* promoter proximal E-box, a feature previously described as a hallmark of c-Myc-regulated genes (Fig. 2*B, top, lane 7*; ref. 13). Reintroducing c-Myc into these cells resulted in binding of c-Myc, the recruitment of RNAPII (Fig. 2*B, top, lanes 1* and *3*) and an increase in the acetylation of histone H3 (AcH3) and H4 (AcH4) at the *H19* E-box (Fig. 2*B, bottom, lanes 1* and *2*). The role of histone acetylation in c-Myc-mediated transcriptional induction of *H19* was further supported by evaluating the effect of the histone deacetylase (HDAC) inhibitor TSA. Treatment with TSA resulted in increased expression of H19 in $myc^{-/-}$ cells as detected by semiquantitative RT-PCR (Fig. 3*A, lanes 1-4*). Curiously, the level of *H19* expression achieved by TSA treatment was higher in $myc^{-/-}$ cells than in c-Myc-expressing cells (Fig. 3*A, lanes 3* and *4*). Thus, histone acetylation activity is recruited by c-Myc to the *H19* promoter, leading to its activation.

c-Myc does not affect imprinting of the *H19/IGF2* locus. Because the paternal allele of *H19* is usually silent due to ICR methylation (see Fig. 1*A*), the effect of DNA methylation on c-Myc regulation of H19 and IGF2 was further investigated. *H19* expression was evaluated in $myc^{-/-}$ cells and c-Myc reconstituted cells in the presence and absence of DNA methylation inhibitor AzaC. Exposure to AzaC did not result in H19 up-regulation in $myc^{-/-}$ cells (Fig. 3*A*, compare *lanes 1, 5*, and *7*), whereas blocking DNA methylation increased *H19* expression in c-Myc-reconstituted cells (Fig. 3*A*, compare *lane 2* with *lanes 6* and *8*). By removing DNA methylation (AzaC) and then increasing histone acetylation (TSA), *H19* expression was potentiated in $myc^{-/-}$ cells (Fig. 3*A*, compare *lanes 1, 3*, and *9*), and no further induction by c-Myc was evident under these conditions (Fig. 3*A, lanes 9* and *10*). Blocking DNA methylation also did not affect IGF2 basal gene expression (Fig. 3*A*, compare *lanes 1, 5*, and *7*) but further potentiated c-Myc repression of this target gene (Fig. 3*A*, compare *lanes 2, 6*, and *8*). c-Myc repression of *IGF2* remains intact despite treatment with both TSA and AzaC (Fig. 3*A, lanes 9* and *10*). These data suggest that c-Myc regulation of the *H19/IGF2* locus does not involve DNA methylation or imprinting. Moreover, loss of methylation alone is insufficient to alter basal gene expression but can cooperate with c-Myc to potentiate the regulation of these target genes.

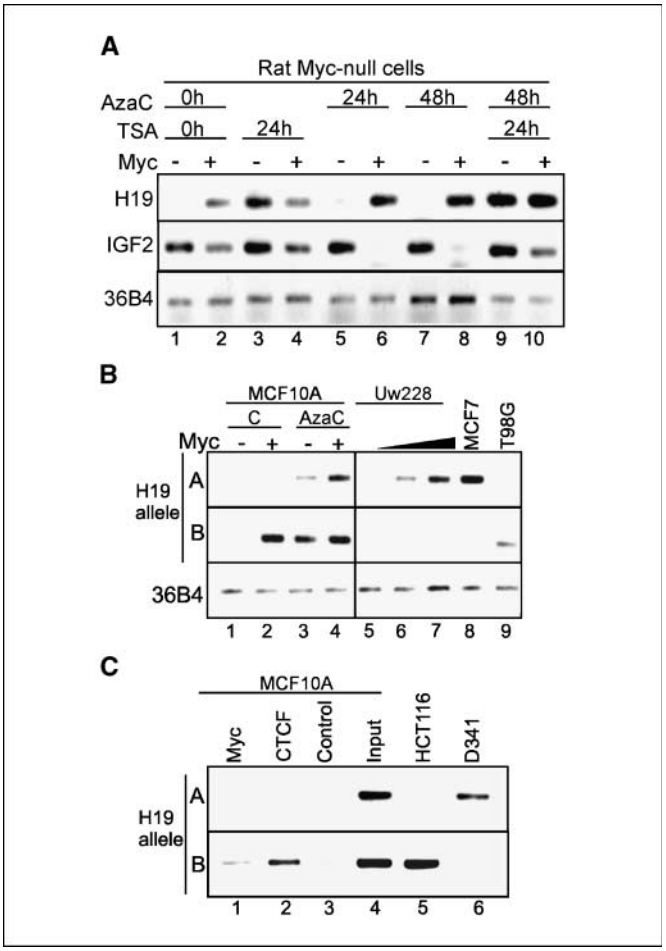

Figure 3. Myc binds and regulates only one allele of H19. *A,* semiquantitative RT-PCR of H19 and IGF2 in Myc null rat fibroblasts expressing the control vector (−) or ectopic Myc (+) that were exposed to HDAC inhibitor TSA and/or DNA methylation inhibitor AzaC for the time indicated. The ribosomal protein 36B4 mRNA serves as a control. Semiquantitative RT-PCR was conducted twice with similar results. *B,* allelic expression analysis of H19 using semiquantitative RT-PCR. *C,* allele-specific binding by Myc and CTCF in MCF10A cells that were used for chromatin immunoprecipitation with Myc-specific and CTCF-specific antibodies, and the immunoprecipitates were analyzed with allele-specific primers. PCR analysis was conducted thrice; representative data are shown.

c-Myc up-regulates only one allele of *H19*. Because the *H19/IGF2* locus is subject to genomic imprinting, we had a unique opportunity to investigate the transcriptional regulatory effect of c-Myc on the allelic expression of *H19*. Multiple cell lines were first tested for polymorphisms in the *H19* locus (data not shown), and the allele-specific primers A and B (*Alu*I polymorphism) were then designed, differing by a 3′ single nucleotide. The primers were tested on the homozygous MCF7 and T98G cells to show allelic specificity (Fig. 3*B, lanes 8* and *9*). In MCF10A cells, ectopic expression of c-Myc induced expression of *H19* from the single allele B (Fig. 3*B, lanes 1* and *2*). c-Myc induction of both alleles of H19 was evident in the presence of AzaC, showing that in the absence of DNA methylation, c-Myc can access and activate both alleles of *H19* (Fig. 3*B, lanes 3* and *4*). Similarly, ectopic expression of increasing amounts of c-Myc activates only the single allele A of *H19* in a dose-dependent manner in Uw228 medulloblastoma cells (Fig. 3*B, lanes 5-7*). Therefore, c-Myc induces *H19* expression by a mechanism that is restricted to only one allele of *H19*.

c-Myc binds to the promoter of one *H19* allele. To further evaluate the molecular mechanism of c-Myc induced allele-specific expression of *H19,* we queried whether c-Myc binds to only one or both alleles of *H19 in vivo*. Allele-specific chromatin immunoprecipitation primers were tested on control DNA from homozygous HCT116 and D341 cell lines to ensure that only one allele is recognized using this approach (Fig. 3*C, lanes 5* and *6*). Both c-Myc and CTCF are bound to allele B but not allele A in MCF10A cells (Fig. 3*C*, compare *lanes 1-3* and *lanes 2-3*). The weaker signal for c-Myc binding could be due to the allele-specific primers being situated 0.4 kb away from the E-box. The bound allele was designated as allele B (Fig. 3*B*) because it has been reported that CTCF binds to the maternally derived, expressed allele of *H19* (26). Indeed, allele B of *H19* is bound by c-Myc and CTCF (Fig. 3*C, lanes 1* and *2*), whereas allele A is not bound by either c-Myc or CTCF, nor it is sensitive to induced expression in response to ectopic c-Myc in MCF10A cells. These allelic binding results were also confirmed by methyl-specific PCR (data not shown). Thus, c-Myc and CTCF bind to the maternally derived, expressed allele of *H19*.

H19 knockdown inhibits tumorigenic properties of breast and lung cancer cells. To assess the role of H19 in transformation, we evaluated the expression and functional significance of H19 in cells derived from breast and lung carcinomas. H19 has recently been reported to be elevated in a high proportion of these tumor types (20, 22). H19 expression was evident in the SKBR3 and T47D breast cancer cell lines and the lung adenocarcinoma A549 cells, whereas expression was undetectable in MDA-MB231 breast cancer cell line (Fig. 4*A*). Stable siRNA-mediated knockdown of H19 resulted in significant decrease in both clonogenicity, as assessed by the efficacy of colony formation on solid support (Fig. 4*B*), and anchorage-independent growth, as assessed by colony formation in soft agar (Fig. 4*C*). The inhibition of both clonogenicity- and anchorage-independent growth in response to H19 knockdown was significant in all cell lines with H19 expression (SKBR3, T47D, and A549), and insignificant in cells with undetectable basal H19 expression, such as MDA-MB231 cells or H460 and H520 lung carcinoma cell lines (Fig. 4*B* and *C*; data not shown). A lack of biological effect of H19 siRNA in MDA-MB231, H460, and H520 serves as an important specificity control. Three of five siRNAs designed worked well to down-regulate H19 expression; however, only one was specific (data not shown). Another siRNA we identified as a nonspecific H19 siRNA was previously used to transiently down-regulate H19 (35). Thus, H19 contributes to the clonogenic and anchorage-independent growth properties in breast and lung cancer cells with reactivated H19 expression.

H19 regulation of IGF2. As H19 has been reported to repress the levels of IGF2, we also monitored the effect of H19 knockdown on IGF2 levels. No significant and consistent increase in IGF2 expression upon H19 repression was noted in any of the breast cancer cells (Fig. 4*D*) or MCF10A cells expressing ectopic c-Myc and elevated H19 (data not shown). Only the A549 cells with H19 knockdown displayed increased IGF2 transcript expression (Fig. 4*D*).

c-Myc binds to the *H19* promoter in SKBR3 but not MDA-MB231 cells. To further evaluate the mechanism of c-Myc induction of *H19* transcription, we queried whether c-Myc was bound to the *H19* E-box (−1.5 kb) in cells with (SKBR3) and without (MDA-MB231) basal *H19* expression. Quantitative chromatin immunoprecipitation analysis showed that c-Myc, CTCF, RNAPII, and AcH4 were present at the *H19* E-box in SKBR3 compared with control antibody (Fig. 5*A*). However, in MDA-MB231 cells, binding of c-Myc and RNAPII was not evident, whereas the binding of CTCF was reduced, and AcH4 was unaffected (Fig. 5*A*). The positive control E-box (CAD) bound c-Myc and RNAPII in both cell lines, whereas the negative control E-box on chromosome 21 had no significant binding of any of the factors (Fig. 5*B* and *C*). Therefore, c-Myc binds to the promoter region of *H19* in SKBR3 cells and contributes to the up-regulation of H19.

High expression levels of H19 correlate with elevated levels of c-Myc mRNA in breast and lung cancer patients. To determine if c-Myc regulation of H19 is a feature of primary human

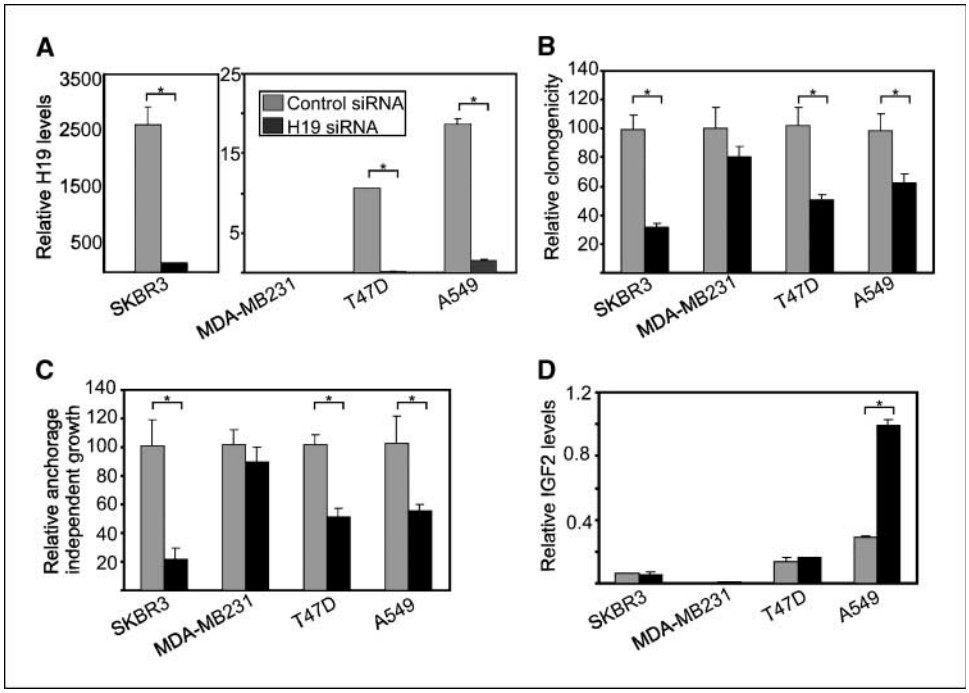

Figure 4. H19 siRNA inhibits cellular transformation. *A,* quantitative RT-PCR assessment of the basal H19 expression and efficacy of H19 siRNA. 36B4 mRNA was used for normalization. The graph of SKBR3 is illustrated separately due to the very high H19 expression. Quantitative RT-PCR was conducted twice in triplicate. *Columns,* mean; *bars,* SD. *, $P < 0.05$, statistical significance as assessed using a paired *t* test. *B,* clonogenicity is decreased in response to the ectopic expression of H19 siRNA in cell lines with basal H19 expression. The experiment was conducted two independent times with consistent results; a representative experiment is shown. Experimental results were normalized between the cell lines. *Columns,* mean; *bars,* SD. *, $P < 0.05$, statistical significance as assessed using a paired *t* test. *C,* anchorage-independent growth is decreased in response to H19 siRNA. Data were analyzed, and significance test was done as in (*B*). *D,* quantitative RT-PCR analysis of IGF2 expression was conducted as in *A*.

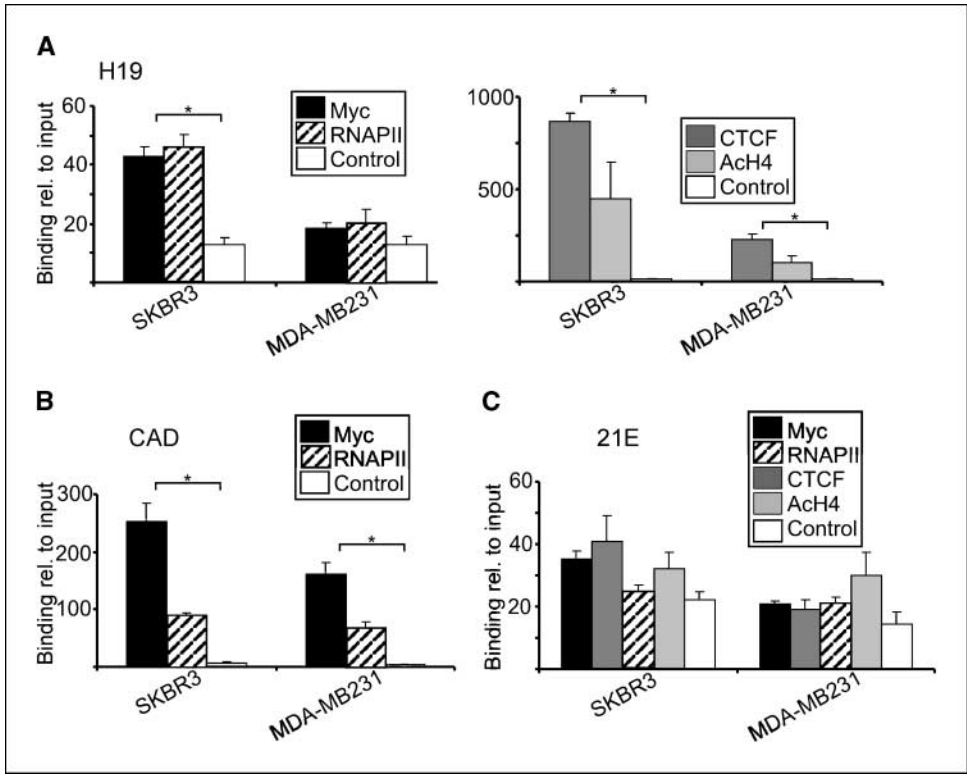

Figure 5. Transcriptional complex binding at the *H19* promoter in SKBR3 and MDA-MB231 cells. *A,* chromatin immunoprecipitation and quantitative PCR analysis of transcriptional components binding the *H19* E-box. *Left,* Myc and RNAPII binding relative to control; *right,* CTCF and AcH4 binding. *B,* chromatin immunoprecipitation and quantitative PCR analysis of Myc and RNAPII binding at the positive control CAD in both cell lines. *C,* chromatin immunoprecipitation and quantitative PCR analysis of negative control E-box binding on chromosome 21. Real-time quantitative PCRs were done and analyzed as in Fig. 2. *, $P < 0.001$, statistical significance as assessed using a *t* test.

tumors, we obtained expression estimates for both genes from a large microarray study of 137 node-negative breast cancer cases. Following data normalization and centering, patients were dichotomized into two equal-sized groups based on H19 expression levels (Fig. 6). Using a two-tailed heteroscedastic *t* test, we show that c-Myc expression was significantly higher ($P = 0.009$) in breast tumors with high H19 levels than those showing lower H19 expression. To show that this is a feature of other tumor types, we characterized the relationship between H19 and c-Myc expression in lung cancers using quantitative RT-PCR in a panel of 240 NSCLCs. Following normalization to a battery of four housekeeping genes, we again dichotomized patients into two equal-sized groups based on H19 expression levels (Fig. 6). Using a two-tailed heteroscedastic *t* test, we again found that c-Myc expression was significantly higher ($P = 0.002$) in tumors with elevated H19 levels than those showing lower H19 expression. To ensure that our results are not artifacts of the statistical analysis, we verified the results using a two-log threshold with the hypergeometric test and again found statistical significance ($P = 0.01$). Both boxplot and spikeplot representations of the data are available as Supplementary Figs. S3 and S4. These analyses show positive correlation of high H19 levels with elevated c-Myc mRNA levels. Selected clinical information is available in Supplementary Tables S4 and S5.

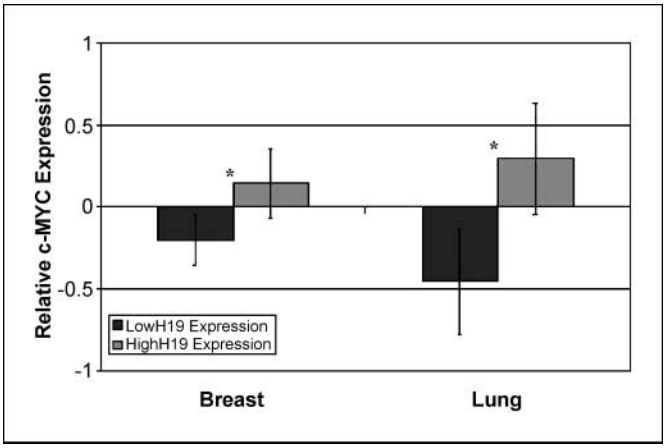

Figure 6. The expression of H19 and c-Myc are related in both breast ($n = 137$) and lung ($n = 240$) tumor samples. For each tumor type, tumors were dichotomized into two equal-sized groups based on H19 expression, and c-Myc expression was compared between the high and low H19 cohorts. *, $P < 0.01$, significance by a two-tailed *t* test. *Columns,* mean; *bars,* 95% confidence intervals.

Discussion

Based on allelic expression and genomic binding studies, we show that c-Myc directly binds to the *H19* promoter and highly up-regulates the transcription of the maternal *H19* allele by recruiting HAT activity. We further show that H19 knockdown, in a panel of breast and lung cancer cell lines, results in the reduction of their tumorigenic phenotype as shown by foci formation and anchorage-independent growth assays. Indeed, a strong association between c-Myc and H19 transcript levels was evident in both primary breast and lung cancer patient material. Taken together, these results indicate that Myc up-regulation of H19 strongly contributes to the tumorigenic phenotype of breast and lung cancer cells.

Our study shows that c-Myc binds to the conserved E-boxes at the *H19* promoter close to the ICR and up-regulates the expression of this ncRNA in MCF10A breast epithelial and established rat fibroblast cell lines. The physical boundary between the ICR and the promoter of *H19* remains undefined; thus, we investigated the mechanism of regulation and show that Myc does not affect ICR

function or imprinting of this locus, as H19 remains expressed from one allele only. In a parallel study, Lee et al. also found that c-Myc up-regulates H19 in mouse liver *in vivo*.[8] However, their data indicate the strongest binding of Myc at an enhancer downstream of the *H19* promoter in hepatocytes. We did not see significant binding of Myc to this region in MCF10A cells expressing ectopic Myc (data not shown). The distinct binding sites and possibly induction mechanisms used by Myc in human and rat transformed cells compared with murine nontransformed hepatocytes is intriguing and likely is a consequence of cell type differences. Importantly, only the maternal allele of *H19* was regulated by Myc in both studies.

Our results show that c-Myc binds and regulates the maternal *H19* allele strongly supporting the observation that the c-Myc/Max complex is unable to bind methylated E-boxes *in vitro* (36). While this article was in preparation, N-Myc was also reported to selectively bind to unmethylated E-boxes (37). This suggests that E-box methylation is a determinant of c-Myc and N-Myc as regulators of gene transcription. This is further supported by our results showing that the silenced paternal allele did not display binding or regulation by Myc in MCF10A cells, whereas removal of DNA methylation leads to induction of the paternal allele by c-Myc. These data suggest that changes in the DNA methylation patterns, which are common in cancer (38), could alter transcriptional profiles and thus modulate the biological function of Myc.

Our results indicating that c-Myc binds and activates *H19* in an allele-specific manner suggests that additional transcription factors, as well as Myc, may regulate transcription with allelic preference. Recent analyses have shown that allelic variation in gene expression is common even in the nonimprinted genes in mammalian genomes and may affect 20% to 50% of human genes (39). We also show that the main function of Myc at the *H19* promoter is to recruit HAT activity and RNAPII for transcriptional initiation. In cells lacking Myc, basal H19 expression was induced only in response to HDAC inhibition but not to the inhibition of DNA methylation. Similarly, the silencing of $p16^{INK4A}$ can also occur in the absence of DNA methylation through histone modifications (40). Therefore, Myc binds the ICR of *H19* in an allele-specific manner to induce transcription through the recruitment of HAT activity.

Furthermore c-Myc down-regulates IGF2 transcripts in cell lines with detectable IGF2 mRNA. Mechanistically, our data indicate that Myc binding is restricted to the maternal allele ICR and is unlikely to have an effect on IGF2 expression from the paternal allele. Although it has been reported that H19 can repress IGF2 expression (41), we did not consistently observe this cross-regulation in the cell systems studied, suggesting this potential regulatory mechanism may be a cell-dependent and/or tumor type–dependent phenomenon. Surprisingly, our data indicate that Myc binds the E-box in the first intron of *IGF2* to repress transcription. Most Myc repressed genes analyzed to date are regulated through initiator or proximal promoter regions (6–8). It remains to be determined whether E-box-dependent Myc repression is evident and unique to IGF2 or functional at multiple loci. Moreover, it remains unclear whether this potentially novel mechanism is best captured through genomic analysis *in vivo* and not detectable by conventional transient indicator gene analysis methods. Biologically, gene expression analysis of a series of neuroblastoma cell lines indicated that high N-Myc levels correlate with low IGF2 levels (42). However, colon carcinomas display high levels of Myc and loss of *IGF2* imprinting (expressed from both alleles) that is sometimes accompanied by elevated levels of IGF2 (43). This implies that the repression of IGF2 is cell specific or is lost in colon cancer cells. At this time, the significance of IGF2 down-regulation by Myc remains unclear. As a mitogen in many cell types, IGF2 is part of a signaling cascade that is able to induce Myc and Myc repression of IGF2 could function as part of negative feedback loop to control mitogen stimulation. A similar function has been proposed for Myc repression of the platelet-derived growth factor-β receptor (7).

The physiologic role of H19 ncRNA seems to be restricted to the time of embryonic expression (44), and its pathologic role has only recently been investigated. The introduction of H19 into some cell lines resulted in anchorage-independent growth suppression, thus earning H19 tumor suppressor designation (18, 19). Recently, however, H19 expression has been shown to be reactivated in a variety of tumors (20–25). Ectopic expression of H19 in MDA-MB231 and T24P cells increased their growth and tumorigenicity (45, 46), whereas the subsequent knockdown of H19 in MDA-MB231 reduced cell proliferation (35). We show that the knockdown of H19 in SKBR3, T47D, and A549 cells leads to the reduction of their clonogenic ability and decreased anchorage-independent growth. The analysis of H19 and c-Myc expression in primary breast and lung tumor samples indicated that high H19 levels are strongly associated with high Myc transcript levels. This strong association in primary tissue, in combination with the essential role of H19 in transformation, suggests that Myc-induced H19 expression contributes to both tumor etiology and Myc's function as an oncogene.

The function of H19 remains enigmatic. Although knockout *H19* mice seem grossly normal (47), we and others show that H19 plays a role in the tumorigenic phenotype (35, 45, 46). Based on the physical association of the H19 transcript with polysomes, the mechanism of H19 action is thought to be at the level of translational regulation (48). In addition, thioredoxin, a modulator of signal transduction and potentiator of tumorigenesis, was recently identified as translationally up-regulated by H19 (49). Further studies will undoubtedly elucidate other H19-regulated molecules and the role of H19 in both physiologic and pathologic settings. As more transcriptional regulators of H19 are determined, H19 regulation and function will also be better understood. Although this work was in progress, E2F1 was shown to regulate *H19* (35), which suggests that Myc and E2F1 can exert a positive combinatorial control over H19 transcription. It is notable that genes bound by Myc (12–15) and E2F1 (50) display a considerable overlap.

We have thus identified *H19* as a Myc-up-regulated gene that potentiates the tumorigenic phenotype of breast and lung cancer cells. Complex interactions between DNA methylation and histone modifications regulate H19 expression, where the role of Myc is to recruit HAT activity to unmethylated E-boxes and initiate allele-specific *H19* transcription.

Acknowledgments

Received 1/6/2006; revised 2/15/2006; accepted 3/9/2006.

Grant support: National Cancer Institute of Canada with funds from the Canadian Cancer Society (L.Z. Penn), Terry Fox Run (I.L. Andrulis), Canadian Institutes of Health Research Scholarships (P.C. Boutros and D. Barsyte-Lovejoy), Institute for Robotics and Intelligent Systems (I. Jurisica). In addition, this research was also supported by the U.S. Department of Defense Breast Cancer Research Program grant BC032138 (L.Z. Penn), as such, the content of the information does

[8] Personal communication.

not necessarily reflect the position or the policy of the Government, and no official endorsement should be inferred.

The costs of publication of this article were defrayed in part by the payment of page charges. This article must therefore be hereby marked *advertisement* in accordance with 18 U.S.C. Section 1734 solely to indicate this fact.

A special thank you to Drs. Linda Lee and Chi Dang (Johns Hopkins University, Baltimore, MD) for communicating unpublished data in advance of publication. We thank Dr. Muthuswamy (Harvard, Boston, MA) for MCF10A cells; Dr. Huang (Hospital for Sick Kids, Canada) for Uw228 cell and their Myc containing derivative cDNA; Drs. Stewart, Novina, and Weinberg (Whitehead, MA) for the lentiviral transfer plasmid; Dr. Naldini (San Raffaele Telethon Institute, Italy) for lentiviral packaging constructs. We especailly indebted to Drs. Mao, Oster, and Katz for technical assistance and S. Colby for breast cancer expression array analysis. We thank the Penn laboratory for constructive discussion and review of the manuscript.

References

1. Nesbit CE, Tersak JM, Prochownik EV. MYC oncogenes and human neoplastic disease. Oncogene 1999;18:3004–16.
2. Oster SK, Ho CS, Soucie EL, et al. The myc oncogene: MarvelouslY Complex. Adv Cancer Res 2002;84:81–154.
3. McMahon SB, Van Buskirk HA, Dugan KA, et al. The novel ATM-related protein TRRAP is an essential cofactor for the c-Myc and E2F oncoproteins. Cell 1998;94:363–74.
4. Cheng SW, Davies KP, Yung E, et al. c-MYC interacts with INI1/hSNF5 and requires the SWI/SNF complex for transactivation function. Nat Genet 1999;22:102–5.
5. Eberhardy SR, Farnham PJ. Myc recruits P-TEFb to mediate the final step in the transcriptional activation of the cad promoter. J Biol Chem 2002;277:40156–62.
6. Barsyte-Lovejoy D, Mao DY, Penn LZ. c-Myc represses the proximal promoters of GADD45a and GADD153 by a post-RNA polymerase II recruitment mechanism. Oncogene 2004;23:3481–6.
7. Mao DY, Barsyte-Lovejoy D, Ho CS, et al. Promoter-binding and repression of PDGFRB by c-Myc are separable activities. Nucleic Acids Res 2004;32:3462–8.
8. Staller P, Peukert K, Kiermaier A, et al. Repression of $p15^{INK4b}$ expression by Myc through association with Miz-1. Nat Cell Biol 2001;3:392–9.
9. Dang CV. c-Myc target genes involved in cell growth, apoptosis, and metabolism. Mol Cell Biol 1999;19:1–11.
10. O'Connell BC, Cheung AF, Simkevich CP, et al. A large scale genetic analysis of c-Myc-regulated gene expression patterns. J Biol Chem 2003;278:12563–73.
11. Watson JD, Oster SK, Shago M, et al. Identifying genes regulated in a Myc-dependent manner. J Biol Chem 2002;277:36921–30.
12. Orian A, van Steensel B, Delrow J, et al. Genomic binding by the Drosophila Myc, Max, Mad/Mnt transcription factor network. Genes Dev 2003;17:1101–14.
13. Mao DY, Watson JD, Yan PS, et al. Analysis of Myc bound loci identified by CpG island arrays shows that Max is essential for Myc-dependent repression. Curr Biol 2003;13:882–6.
14. Li Z, Van Calcar S, Qu C, et al. A global transcriptional regulatory role for c-Myc in Burkitt's lymphoma cells. Proc Natl Acad Sci U S A 2003;100:8164–9.
15. Fernandez PC, Frank SR, Wang L, et al. Genomic targets of the human c-Myc protein. Genes Dev 2003;17:1115–29.
16. Cawley S, Bekiranov S, Ng HH, et al. Unbiased mapping of transcription factor binding sites along human chromosomes 21 and 22 points to widespread regulation of noncoding RNAs. Cell 2004;116:499–509.
17. Costa FF. Non-coding RNAs: new players in eukaryotic biology. Gene 2005;357:83–94.
18. Hao Y, Crenshaw T, Moulton T, et al. Tumour-suppressor activity of H19 RNA. Nature 1993;365:764–7.
19. Isfort RJ, Cody DB, Kerckaert GA, et al. Role of the H19 gene in Syrian hamster embryo cell tumorigenicity. Mol Carcinog 1997;20:189–93.
20. Adriaenssens E, Dumont L, Lottin S, et al. H19 overexpression in breast adenocarcinoma stromal cells is associated with tumor values and steroid receptor status but independent of p53 and Ki-67 expression. Am J Pathol 1998;153:1597–607.
21. Tanos V, Ariel I, Prus D, et al. H19 and IGF2 gene expression in human normal, hyperplastic, and malignant endometrium. Int J Gynecol Cancer 2004;14:521–5.
22. Kondo M, Suzuki H, Ueda R, et al. Frequent loss of imprinting of the H19 gene is often associated with its overexpression in human lung cancers. Oncogene 1995;10:1193–8.
23. Douc-Rasy S, Barrois M, Fogel S, et al. High incidence of loss of heterozygosity and abnormal imprinting of H19 and IGF2 genes in invasive cervical carcinomas. Uncoupling of H19 and IGF2 expression and biallelic hypomethylation of H19. Oncogene 1996;12:423–30.
24. Hibi K, Nakamura H, Hirai A, et al. Loss of H19 imprinting in esophageal cancer. Cancer Res 1996;56:480–2.
25. Ariel I, Sughayer M, Fellig Y, et al. The imprinted H19 gene is a marker of early recurrence in human bladder carcinoma. Mol Pathol 2000;53:320–3.
26. Reik W, Walter J. Genomic imprinting: parental influence on the genome. Nat Rev Genet 2001;2:21–32.
27. Macleod D, Ali RR, Bird A. An alternative promoter in the mouse major histocompatibility complex class II I-Abeta gene: implications for the origin of CpG islands. Mol Cell Biol 1998;18:4433–43.
28. Debnath J, Muthuswamy SK, Brugge JS. Morphogenesis and oncogenesis of MCF-10A mammary epithelial acini grown in three-dimensional basement membrane cultures. Methods 2003;30:256–68.
29. Oster SK, Mao DY, Kennedy J, et al. Functional analysis of the N-terminal domain of the Myc oncoprotein. Oncogene 2003;22:1998–2010.
30. Chomczynski P, Sacchi N. Single-step method of RNA isolation by acid guanidinium thiocyanate-phenol-chloroform extraction. Anal Biochem 1987;162:156–9.
31. Andrulis IL, Bull SB, Blackstein ME, et al. neu/erbB-2 amplification identifies a poor-prognosis group of women with node-negative breast cancer. Toronto Breast Cancer Study Group. J Clin Oncol 1998;16:1340–9.
32. Yang YH, Dudoit S, Luu P, et al. Normalization for cDNA microarray data: a robust composite method addressing single and multiple slide systematic variation. Nucleic Acids Res 2002;30:e15.
33. Smyth GK. Linear models and empirical Bayes methods for assessing differential expression in microarray experiments. Statistical Applications in Genetics and Molecular Biology 2003;3:1–26.
34. Paddison PJ, Caudy AA, Bernstein E, et al. Short hairpin RNAs (shRNAs) induce sequence-specific silencing in mammalian cells. Genes Dev 2002;16:948–58.
35. Berteaux N, Lottin S, Monte D, et al. H19 mRNA-like noncoding RNA promotes breast cancer cell proliferation through positive control by E2F1. J Biol Chem 2005;280:29625–36.
36. Prendergast GC, Ziff EB. Methylation-sensitive sequence-specific DNA binding by the c-Myc basic region. Science 1991;251:186–9.
37. Perini G, Diolaiti D, Porro A, et al. *In vivo* transcriptional regulation of N-Myc target genes is controlled by E-box methylation. Proc Natl Acad Sci U S A 2005;102:12117–22.
38. Jones PA, Baylin SB. The fundamental role of epigenetic events in cancer. Nat Rev Genet 2002;3:415–28.
39. Yan H, Yuan W, Velculescu VE, et al. Allelic variation in human gene expression. Science 2002;297:1143.
40. Bachman KE, Park BH, Rhee I, et al. Histone modifications and silencing prior to DNA methylation of a tumor suppressor gene. Cancer Cell 2003;3:89–95.
41. Wilkin F, Paquette J, Ledru E, et al. H19 sense and antisense transgenes modify insulin-like growth factor-II mRNA levels. Eur J Biochem 2000;267:4020–7.
42. Raetz EA, Kim MK, Moos P, et al. Identification of genes that are regulated transcriptionally by Myc in childhood tumors. Cancer 2003;98:841–53.
43. Kaneda A, Feinberg AP. Loss of imprinting of IGF2: a common epigenetic modifier of intestinal tumor risk. Cancer Res 2005;65:11236–40.
44. Brannan CI, Dees EC, Ingram RS, et al. The product of the H19 gene may function as an RNA. Mol Cell Biol 1990;10:28–36.
45. Lottin S, Adriaenssens E, Dupressoir T, et al. Overexpression of an ectopic H19 gene enhances the tumorigenic properties of breast cancer cells. Carcinogenesis 2002;23:1885–95.
46. Ayesh S, Matouk I, Schneider T, et al. Possible physiological role of H19 RNA. Mol Carcinog 2002;35:63–74.
47. Jones BK, Levorse JM, Tilghman SM. Igf2 imprinting does not require its own DNA methylation or H19 RNA. Genes Dev 1998;12:2200–7.
48. Li YM, Franklin G, Cui HM, et al. The H19 transcript is associated with polysomes and may regulate IGF2 expression in trans. J Biol Chem 1998;273:28247–52.
49. Lottin S, Vercoutter-Edouart AS, Adriaenssens E, et al. Thioredoxin post-transcriptional regulation by H19 provides a new function to mRNA-like non-coding RNA. Oncogene 2002;21:1625–31.
50. Weinmann AS, Yan PS, Oberley MJ, et al. Isolating human transcription factor targets by coupling chromatin immunoprecipitation and CpG island microarray analysis. Genes Dev 2002;16:235–44.